THE CALCULATION OF THE BENDING MOMENT RESPONSE OF A TYPICAL LAUNCH VEHICLE USING GENERALIZED POWER SPECTRAL TECHNIQUES

by

W. C. Lennox
F. P. Beer

February 15, 1966

Research Grant
No. NsG-466
National Aeronautics and Space Administration

Institute of Research
Lehigh University
Bethlehem, Pennsylvania

TABLE OF CONTENTS

Abstract 3

Symbols 4

1. Introduction 5

2. Analysis 9

3. Vehicle Response Functions 15

4. Vehicle Parameters 17

5. Linearity Check 17

6. Input Data 18

7. Results 19

8. Acknowledgement 19

Appendix A - Simplification for Computing Fourier Transforms 20

Appendix B - Equations for Typical Vehicle 22

Appendix C - Numerical Fourier Transforms 33

References 38

Figures 41

Tables 51

ABSTRACT

23745

The concepts of frequency response and power spectrum, so well-known in the aircraft industry, are extended to the problem of obtaining the statistics of the rigid-body bending moment response of a typical vehicle as it rises through the atmosphere. The mean and standard deviation of the response at the "critical" altitude are obtained utilizing wind statictics collected at Cape Kennedy, Florida. Essentially the method is based upon the computation of the response of the vehicle to sinusoidal wind profiles of various wave-numbers and upon the generalized power spectrum of the wind velocity. Under the assumption that the response is Gaussian, extreme-value bending moment loads are estimated which would be useful for preliminary design purposes.

SYMBOLS

$h^n(z',z)$	impulse response function
$H^n(z;k)$	frequency response function
k	wave-number
$q^n(z)$	bending-moment at station n
$Q^n(z;k)$	complex response function of vehicle to sinusoidal input e^{ikz}
$Q^n_{cos}(z;k)$	response of the vehicle to a cosine wind-velocity profile
$Q^n_{sin}(z;k)$	response of the vehicle to a sine wind-velocity profile
$u(z)$	wind-velocity
$U(k)$	Fourier transform of u(z)
δ	Dirac delta function
ρ	correlation coefficient
σ	standard deviation
$\mathscr{C}_{qq}$	response covariance function
$\mathscr{C}_{uu}$	wind-velocity covariance function
Φ_{uu}	wind-velocity generalized power spectral density function
$< >$	expected value of
$[\ ]$	matrix
$[\ ]^T$	transpose of matrix

I. INTRODUCTION

To insure a feasible design for the primary structure of an aerospace vehicle, an engineer must have available analytical methods for estimating beforehand the loads that may be induced in the vehicle during flight. The loads of particular concern here will be the bending moment loads induced in the vehicle as it rises through its environment of random wind disturbances.

Usually in order to obtain a preliminary estimate, a digital computer is programmed to simulate the flight of the vehicle as it "flies" through a wind profile or a series of profiles. The profiles used may be real[1] or they may be synthetic, that is, they may be based on observed extreme wind conditions without actually representing any of the observed profiles[2,3]. It should be noted that the latter approach is the subject of considerable controversy because of the difficulty of selecting or deriving a "critical" profile. In order to obtain more detailed load statistics, a method called the "statistical load survey" is then employed[4]. Essentially, a large number of representative wind profiles are assembled and, for each of these, the corresponding response of the vehicle is computed. Response statistics are then estimated from an analysis of the resulting response records.

While this method is straightforward, it is relatively expensive as it requires considerable time to carry out enough computer calculations to accumulate a sufficient "statistical sample". Also, nothing may be inferred about loads which were not achieved. In a previous paper[5], the authors indicated this shortcoming and proposed a method which makes a more effective use of the results of a "statistical load survey". If certain requirements are satisfied, this method makes it possible to obtain the statistics of loads that were never achieved in the sample. Also, methods were proposed by which the use of a statistical load survey may be avoided altogether. Under the assumption that the vehicle constitutes a linear system, it was shown how the response statistics of the vehicle may be obtained from the wind field statistics and the equations describing the vehicle. Various methods were proposed, utilizing the concepts of impulse response functions, system adjoint functions, and frequency response functions to describe the system, while covariance functions and generalized power spectral density functions were used to describe the wind field.

The purpose of this paper is to apply one of the suggested methods to a typical launch vehicle. The method to be presented utilizes frequency concepts, that is, it characterises the vehicle by means of frequency response functions and the random input field by means of power

spectra. Since the wind-velocity field is a nonstationary (nonuniform space-wise) field, a generalized power spectral density function must be used. Also, since the coefficients of the equations defining the system are space-dependent, a space-dependent frequency response function is required.

Power spectral techniques have been applied quite successfully to the problem of determining the dynamic response of aircraft to atmospheric turbulence for a period of over ten years. It evolved quite naturally, since turbulence is a random process, as an alternative to the discrete-gust approach and is used at present in conjunction with discrete-gust analysis. To quote Reference 6, "the main assets offered by the power spectral approach are as follows:

1. It allows for a more realistic representation of the continuous nature of atmospheric turbulence.

2. It allows airplane configurations and response characteristics to be taken into account in a rational manner.

3. It allows more rational consideration of design and operational variations such as configuration changes, mission changes, and airplane degrees of freedom".

It is felt that perhaps some of the above-mentioned assets may be equally valid when the system under consideration is a launch vehicle. Discrete-wind profile methods already are being used in industry. As methods of wind measurement become more refined, allowing wind shear and atmospheric turbulence to be considered jointly, so should the techniques used to estimate the response of the vehicle.

As an illustrative example, the mean and variance of the rigid-body bending moment are computed at five locations on a typical launch vehicle, as the vehicle passes through the critical altitude of 36,000 feet. This altitude corresponds to the point of maximum dynamic pressure and it is also the altitude at which the vehicle recovers from the large wind shear reversal which characterizes the wind profile in the area of Cape Kennedy where the wind data was collected. It is thus the altitude at which the vehicle response may be expected to be maximum. The motion is constrained to the pitch plane and the analysis uses only the dominant (East-West) component of the wind field. It should be noted that the assumptions made regarding the launch vehicle are consistent with the methods of analysis used today. The omission of the elastic modes may be justified by the predominance of the rigid body modes in the structural load response of large and relatively stiff vehicles to wind disturbances.

Under the assumption that the wind velocity is Gaussian, extreme-value design loads are computed. It is felt that the results obtained should be useful for preliminary design.

2. ANALYSIS

Let $q^n(z)$ represent the bending moment induced in the launch vehicle at station n, located along the axis of the vehicle, when the vehicle is at height z (Figure 1). Since the system is assumed to be linear, $q^n(z)$ is defined as the solution of the following linear differential equation:

$$L\, q^n(z) = u(z) \tag{1}$$

where L represents a linear differential operator with z-dependent coefficients and u(z) represents the wind-velocity profile. It is well-known in the theory of linear systems that the solution of Eq. (1) may be expressed as a convolution:

$$q^n(z) = \int_0^z h^n(z',z)\, u(z')\, dz' \tag{2}$$

of the wind profile and of the function $h^n(z',z)$ which represents the solution of:

$$L\, q^n(z) = \delta(z-z') \tag{3}$$

The function $\delta(z-z')$ is the Dirac delta function and represents a unit wind impulse at height z'. The corresponding

response $h(z'z)$ will be referred to as the impulse response function of the vehicle.

The mean value of the response of the vehicle at height z is obtained by averaging both members of Eq. (2) over the ensemble of flights considered.

$$\langle q^n(z)\rangle = \int_0^z h^n(z',z)\ \langle u(z')\rangle\ dz' \qquad (4)$$

Note that the mean response $\langle q^n(z)\rangle$ may be computed as the response of the vehicle to the mean wind velocity $\langle u(z)\rangle$.

The covariance function of the response, defined as

$$\varphi^n_{qq}(z_1,z_2) = \langle (q^n(z_1)-\langle q^n(z_1)\rangle)(q^n(z_2)-\langle q^n(z_2)\rangle)\rangle \qquad (5)$$

is obtained by subtracting Eq. (4) from Eq. (2), member by member, and substituting the result into Eq. (5)

$$\varphi_{qq}(z_1,z_2) = \int_0^{z_1}\int_0^{z_2} h^n(z_1',z_1)h^n(z_2',z_2)\ \varphi_{uu}(z_1',z_2')dz_1'dz_2' \qquad (6)$$

where φ_{uu} is the covariance function of the wind-velocity field. The variance of the response at height z would be obtained by setting $z_1=z_2=z$ in Eq. (6). Thus, Eqs. (4) and (6) represent the solution of the problem and this is

essentially the method used by Bieber[7]. However, as suggested in our previous paper[5], the use of frequency response functions, instead of impulse response functions, may result in a reduction of the required computations, thus saving valuable computer time. Also, it may help to visualize the system better since it is felt that frequency concepts are more familiar to people involved with aerospace systems. Thus, we presented an alternative method that is based upon the computation of the response of the vehicle to sinusoidal wind profiles of various wave-numbers k. Setting

$$u(z) = e^{ikz} \tag{7}$$

in Eq. (1), the following set of differential equations is obtained

$$L\, q^n(z) = e^{ikz} \tag{8}$$

which define the desired responses. Denoting the solutions of Eq. (8) by $Q^n(z;k)$, the frequency response function $H^n(z;k)$ is defined by the relation

$$Q^n(z;k) = H^n(z;k)\, e^{ikz} \tag{9}$$

Note that, contrary to the case of a system characterized by a differential operator with constant coefficients, the frequency response function of the vehicle depends upon the height z.

Substituting for u(z) from Eq. (7) into Eq. (2), the following relation between the function $Q^n(z;k)$ and the impulse response function is obtained

$$Q^n(z;k) = \int_0^z h^n(z',z)\, e^{ikz'}\, dz' \tag{10}$$

and, by dividing both members of Eq. (10) by e^{ikz}, the corresponding relation between the frequency response function and the impulse response function is obtained

$$H^n(z;k) = \int_0^z h^n(z',z)\, e^{-ik(z-z')}\, dz' \tag{11}$$

which is the usual definition of a frequency response function . Note that Q^n is a complex function and may be rewritten as

$$Q^n(z;k) = Q^n_{cos}(z;k) + i\, Q^n_{sin}(z;k) \tag{12}$$

where, using Eq. (10),

$$Q^n_{cos}(z;k) = \int_0^z h(z',z) \cos kz'dz' \tag{13a}$$

and

$$Q^n_{sin}(z;k) = \int_0^z h(z',z) \sin kz'dz' \tag{13b}$$

The functions Q^n_{cos} and Q^n_{sin} represent the response of the vehicle at station n to a cosine and a sine wind-velocity profile, respectively.

To express the mean response of the vehicle in terms of the function $Q^n(z;k)$, we first take the Fourier transform of the mean wind velocity

$$U(k) = \int_0^\infty \langle u(z) \rangle \, e^{-ikz} \, dz \tag{14}$$

and substitute for $\langle u(z) \rangle$ into Eq. (4) the inverse transform

$$\langle u(z) \rangle = (1/2\pi) \int_{-\infty}^{\infty} U(k) \, e^{ikz} \, dk \tag{15}$$

Noting Eq. (10), we obtain the expression

$$\langle q^n(z) \rangle = (1/2\pi) \int_{-\infty}^{\infty} Q^n(z;k) \, U(k) \, dk \tag{16}$$

for the mean response of the vehicle. However, since $u(z)=0$ for $z<0$ it is possible to simplify Eq. (16) with the result that (see Appendix A)

$$\langle q^n(z) \rangle = (2/\pi) \int_0^\infty Q^n_{cos}(z;k) \, \mathrm{Re} \, U(k) \, dk \tag{17}$$

where Re denotes the real part of the function.

In order to use frequency concepts to obtain the variance of the response, we replace the wind-velocity covariance function by its generalized power spectral density function. This is defined as the double Fourier transform of $\mathscr{C}_{uu}$:

$$\Phi_{uu}(k_1,k_2) = \int_0^\infty\int_0^\infty \mathcal{C}_{uu}(z_1,z_2)\, e^{i(k_1z_1-k_2z_2)}\, dz_1dz_2 \qquad (18a)$$

and the inverse relation is

$$\mathcal{C}_{uu}(z_1,z_2) = (1/2\pi)^2 \int_{-\infty}^\infty\int_{-\infty}^\infty \Phi_{uu}(k_1,k_2)e^{i(k_2z_2-k_1z_1)}dk_1dk_2 \qquad (18b)$$

Substituting for $\mathcal{C}_{uu}$ from Eq. (18b) into Eq. (6), we obtain, after using Eq. (10), the following expression for the response covariance function

$$\mathcal{C}^n_{uu}(z_1,z_2)=(1/2\pi)^2\int_{-\infty}^\infty\int_{-\infty}^\infty Q^{n*}(z_1;k_1)Q^n(z_2;k_2)\Phi_{uu}(k_1,k_2)dk_1dk_2 \qquad (19)$$

where Q^{n*} is the conjugate function of Q^n. Thus the variance of the bending moment at station n as a function of height is given by

$$\mathcal{C}^n_{qq}(z,z)=(1/2\pi)^2\int_{-\infty}^\infty\int_{-\infty}^\infty Q^{n*}(z;k_1)Q^n(z;k_2)\Phi_{uu}(k_1,k_2)dk_1dk_2 \qquad (20)$$

However, by using an argument similar to that presented in Appendix A for a Fourier transform in one variable, when $u(z)=0$, $z<0$, Eq. (18b) may be simplified with the result

$$\mathcal{C}_{qq}(z_1,z_2)=(2/\pi)^2\int_0^\infty\int_0^\infty \mathrm{Re}\ \Phi_{uu}(k_1,k_2)\ \cos\ (k_2z_2-k_1z_1)dk_1dk_2 \qquad (21)$$

so that Eq. (20) becomes, noting Eqs. (13),

$$\varphi^n_{qq}(z,z) = (2/\pi)^2 \int_0^\infty\int_0^\infty [Q^n_{cos}(z;k_1)\, Q^n_{cos}(z;k_2)$$

$$+ Q^n_{sin}(z;k_1)\, Q^n_{sin}(z;k_2)]\ \mathrm{Re}\ \Phi_{uu}(k_1,k_2)dk_1dk_2 \quad (22)$$

where Re denotes the real part of the function. In matrix notation, Eqs. (17) and (22) become

$$\langle q^n(z)\rangle = (2\Delta k/\pi)\ [Q^n_{cos}]\ [\mathrm{Re}\ F]^T \quad (23)$$

and

$$\varphi^n_{qq}(z,z)=(2\Delta k/\pi)^2([Q^n_{cos}][\mathrm{Re}\ \Phi_{uu}][Q^n_{cos}]^T+[Q^n_{sin}][\mathrm{Re}\ \Phi_{uu}][Q^n_{sin}]^T) \quad (24)$$

Eqs. (17) and (22) or, alternatively, Eqs. (23) and (24) provide the solution of the bending moment response problem.

3. VEHICLE RESPONSE FUNCTIONS

As indicated by Eqs. (17) and (22), it is necessary to compute the functions Q^n_{cos} and Q^n_{sin}, i.e., the response of the vehicle to cosine and sine wind-velocity profiles. This was accomplished by utilizing an existing high-speed computer program (Langley Program P6382) and the computer facilities (IBM 7094 computer) at Langley Research Center, Virginia. A detailed description of the typical launch vehicle considered, equations of motion, and computer

program is given in Reference 1. However this program takes into account structural flexibility and propellant slosh. These were neglected and only the rigid-body degrees of freedom were retained. A discussion and summary of these equations are given in Appendix B. It should be noted that the equations of motion are nonlinear and have variable coefficients. However, owing to the linearized control system and the small motions involved, the bending moment response is essentially linear. To verify this a linearity check was performed.

The wind velocity is assumed to have the form

$$u(z) = \begin{cases} \sin kz \\ \cos kz \end{cases} \qquad k = \frac{2\pi\kappa}{L} \tag{25}$$

where L is set equal to the terminal altitude, that is, L=60,000 feet. Thus the response of the system to the above expressions will be

$$q^n(z) = \begin{cases} Q^n_{\sin}(z,k) \\ Q^n_{\cos}(z,k) \end{cases} \tag{26}$$

Note that these are functions of z for fixed k. Since the variable of integration in Eqs. (17) and (22) is k, it is necessary to compute a number of functions Q^n for various

values of k and cross-plot the results. Figures 2a and 2b show typical bending moment responses $q^n(z)$ for a fixed value of k. Figure 3 shows the result of the cross-plot yielding a function of k for fixed z. The interpolation was accomplished by means of a second-order interpolation routine.

4. VEHICLE PARAMETERS

Data for a zero-wind vertical ascent are presented in Figure 4; time-histories for the dynamic pressure and Mach number are shown in part (a). As shown in part (b) of Figure 4 the vehicle was flown to a terminal altitude of 60,000 feet which is well beyond the maximum dynamic pressure condition. All data is based on a vertical flight-attitude program (Figure 4c). A normal aerodynamic lift distribution was assumed in the form shown in Figure 5. At launch the vehicle has a thrust to weight ratio of 1.25.

5. LINEARITY CHECK

By definition the system is linear if, for all combinations of u_1 and u_2, the input u_1+u_1 produces the output q_1+q_2. Consequently, the missile system was subjected to inputs of the form $u=C \sin kz$ where the constant was given various different values. For inputs of this form, the bending moment response was found to be essentially linear

throughout the region of interest (Table 1 gives the results for station 2 where the maximum loads occurred).

6. INPUT DATA

The mean and covariance function used for this sample computation were obtained from Reference 8 for Patrick AFB/Cape Kennedy, Florida. This report provides tabulated data on the arithmetic means, standard deviations, and correlations of the meridional (North-South) and zonal (East-West) components of the wind at intervals of one kilometer for six geographic locations. The statistical data is computed from observations obtained over a period of seven years (1951-1957). For this calculation the annual statistics of the East-West component are used. These are given in Table 2 and Table 3. Table 2 shows the average and standard deviation of the E-W winds. Table 3 shows the correlation coefficients of the E-W winds. The covariance function is computed by using the relation

$$\varphi_{uu}(z_1,z_2) = \rho_{uu}(z_1,z_2)\ \sigma_u(z_1)\ \sigma_u(z_2) \qquad (27)$$

where ρ_{uu} is the correlation coefficient and σ_u is the standard deviation of the field u. However, as indicated by Eqs.(17), (22), (14), and (18a), what is required is the Fourier transforms of these functions. Since the available data is not continuous, an approximate numerical procedure

is used (Appendix C). It should be noted that methods for obtaining continuous wind profiles are under current investigation and should soon be available.

7. RESULTS

The results of the previous analysis are presented in Figure 8. The mean and standard deviation of the structural bending moment are given for the 5 stations when the vehicle is at the height of 36,000 feet.

Assuming that the response is normally distributed, extreme value loads are computed by noting that the variable

$$\frac{q^n(z) - \langle q^n(z) \rangle}{\sqrt{d_{11}(z)}}$$

is normally distributed with mean 0 and variance 1. Thus the required statistics may be found in any set of mathematical tables. These results are shown in Figure 9.

8. ACKNOWLEDGEMENT

The authors wish to thank Mr. H. Lester, Aerospace Technologist, NASA Langley Research Center, Virginia, for providing pertinent data required for the solution of the problem.

APPENDIX A

SIMPLIFICATION FOR COMPUTING FOURIER TRANSFORMS

In order to obtain the results indicated in Eqs. (17) and (22) we shall first consider the computation of the Fourier transform of a function u(z) where

$$u(z) = 0 \qquad z<0 \tag{A-1}$$

The Fourier transform pair is given by

$$U(k) = \int_0^\infty u(z)\ e^{-ikz}\ dz \tag{A-2}$$

and

$$u(k) = \frac{1}{2\pi} \int_{-\infty}^{\infty} U(k)\ e^{ikz}\ dk \tag{A-3}$$

However, in view of Eq. (A-1) it may be verified that Eq. (A-3) reduces to[9]

$$u(z) = \frac{2}{\pi} \int_0^\infty \mathrm{Re}\ U(k) \cos kz\ dk \tag{A-4}$$

where Re denotes the real part of the function.

Substituting now for u(z') from (A-4) into Eq. (4), and comparing Eqs. (14) and (A-2), we obtain

$$\langle q^n(z) \rangle = \int_0^z h^n(z',z)\ \langle u(z') \rangle\ dz' \tag{A-5}$$

$$= \int_0^z h^n(z',z)[(2/\pi) \int_0^\infty \text{Re } U(k) \cos kz'dk]\, dz' \qquad \text{(A-6)}$$

$$= \frac{2}{\pi} \int_0^\infty [\int_0^z h^n(z',z) \cos kz'dz'] \text{ Re } U(k)\, dk \qquad \text{(A-7)}$$

which becomes, in view of Eq. (13a),

$$\langle q^n(z) \rangle = (2/\pi) \int_0^\infty Q^n_{\cos}(z;k) \text{ Re } U(k)\, dk \qquad \text{(A-8)}$$

which is the desired result.

A similar analysis may be carried out for a double Fourier transform of $\varphi(z_1,z_2)$ where

$$\varphi(z_1,z_2) = 0 \qquad z_1<0$$

$$\varphi(z_1,z_2) = 0 \qquad z_2<0$$

in order to obtain Eq. (22).

APPENDIX B

EQUATIONS FOR TYPICAL VEHICLE

This section provides a brief discussion of the equations required for the solution of the sample problem. It should be noted that the typical launch vehicle considered, equations of motions, and computer program used for the calculations are similar to those described in Reference 1 with the exception that only the rigid-body degrees of freedom were retained (structural flexibility and propellant slosh were neglected) and the autopilot and gimbaled engine equations were appropriately simplified.

Mathematical Model

The coordinate systems to be used are illustrated in Figure 6. Both body-fixed and inertial (space-fixed) axes are used. In general, motion is referenced to a Cartesian coordinate frame fixed in the rigid body and oriented with respect to the local horizontal by the attitude angle θ. The velocity vector of the center of gravity is oriented to the local horizontal by γ, the flight-path angle, and the rigid-body motion is characterized by translatory motion along the respective body axes and a rotation about the center of gravity. The vehicle is assumed to be autopilot

controlled and subjected to the disturbing influence of the atmospheric winds (in this case, cosine and sine wind profiles). Control forces are produced by gimbaling the thrust chambers of the rocket engines an angle δ in response to commands provided by the autopilot.

Equations of Motion

The equations of motion are derived using a variational principle that is developed from momentum considerations[10]; the equations are

$$\frac{d}{dt}\left(\frac{\partial L}{\partial \dot{\beta}_i}\right) - \frac{\partial L}{\partial \beta_i} = Q_{\beta_i} + \bar{Q}_{\beta_i} \qquad \text{(B-1)}$$

where L is the Lagrangian and β_i is any generalized coordinate. The generalized forces Q_{β_i} and $\bar{Q}_{\beta_i}$ result from external forces not derivable from a potential and internal forces due to mass flow within the system, respectively. It should be noted that while Eqs. (B-1) have the same form as Lagrange's equations, they are derived from a variational principle which does not require the assumption of constant mass, whereas the classical derivation of Lagrange's equations does.

The general form of the Lagrangian operator in Eqs. (B-1) is referred to the space-fixed frame. Since the

motion of the vehicle is referred to the body-fixed frame, it is necessary to transform Eqs. (B-1) to a form that is valid in the rotating system. Details of this transformation to "quasi-coordinates" may be found in Reference 11. When transformed, "Lagrange's" equations assume the following forms:

$$\frac{d}{dt}\left(\frac{\partial T}{\partial \dot{x}_o}\right) - \dot{\theta}\left(\frac{\partial T}{\partial \dot{y}_o}\right) + \sin\theta\left(\frac{\partial U}{\partial h}\right) = \sum F_x$$

$$\frac{d}{dt}\left(\frac{\partial T}{\partial \dot{y}_o}\right) + \dot{\theta}\left(\frac{\partial T}{\partial \dot{x}_o}\right) + \cos\theta\left(\frac{\partial U}{\partial h}\right) = \sum F_y \qquad \text{(B-2)}$$

$$\frac{d}{dt}\left(\frac{\partial T}{\partial \dot{\theta}}\right) + \dot{x}_o\left(\frac{\partial T}{\partial \dot{y}_o}\right) - \dot{y}_o\left(\frac{\partial T}{\partial \dot{x}_o}\right) + \frac{\partial U}{\partial \theta} = \sum M_{c.g.}$$

where T and U represent the kinetic and potential energies, respectively, of the launch vehicle. The generalized forces account for all external forces and moments not included in the potential function U.

The details of forming the kinetic and potential energies may be found in Reference 1. The equations which result from these operations are summarized at the end of this section.

Aerodynamic Considerations

Aerodynamic forces are found by using the quasi-steady method discussed in Reference 12. This method makes use of steady-state lift distributions determined experimentally. Hence, quasi-steady aerodynamic forces are Mach number dependent but only approximate the unsteady effects. Since the aerodynamic data available for the sample vehicle consisted of the total normal-force and pitching moment coefficient $C_{N_\alpha}(M)$ and $C_{m_\alpha}(M)$ as presented in Figure 7, an assumed normal aerodynamic lift distribution was required. This is illustrated in Figure 5b. The constants C_1 and C_2 were determined so that the assumed distribution produces C_{N_α} and C_{m_α}. The afterbody lift was approximated by an exponential variation; the forebody lift was assumed linear.

Bending Moments

The bending moment acting at any point along the structure of the vehicle was determined by the loads summation method as discussed in Reference 13. Application of the method requires finding the lateral load per unit length and integrating to find the resultant bending moment.

Symbols and Equations

(As presented in Langley Working Paper-98 by H.C. Lester, "A Digital Program for Computing Rigid-Body Launch Vehicle Wind Loads, Langley Program P6382")

$a_o(t)$	control system gain
$a_y(t)$	lateral acceleration sensed by an accelerometer located at coordinate x_a, ft/sec^2
$[BM(t)]_n$	bending moment at coordinate x_n, ft-lb
$C_a(M)$	axial-force coefficient
$C_{N_\alpha}(M)$	slope of normal-force coefficient, $\int_0^L C_{n_\alpha}(x,M)dx$, radian^{-1}
$C_{m_\alpha}(M)$	slope of pitching-moment coefficient, $\int_0^L (x-x_{cg})\, C_{n_\alpha}(x,M)dx$, ft/radian
$C_{n_\alpha}(x,M)$	slope of the local normal-force coefficient, 1/ft-radian
F_x, F_y	force in x and y direction, respectively, lb
g	gravitational acceleration constant, ft/sec^2
h(t),r(t)	altitute and range, ft
$I_{c.g.}(t)$	mass moment of inertia of launch vehicle about center of gravity. lb-sec^2-ft
L	Length of launch vehicle, ft
$M_{c.g.}$	pitching moment about center of gravity, ft-lb
M(t)	Mach number, equal to V_{mw}/V_s
$M_t(t)$	total mass of launch vehicle, lb-sec^2/ft

$m(x,t)$	distributed mass of launch vehicle, lb-sec^2/ft
$P_o(h)$	atmospheric pressure at altitude h, lb/ft^2
$q(t)$	dynamic pressure, lb/ft^2
S_o	aerodynamic reference area, ft^2
$T_t(h), T_l(h)$	total thrust of all engines and gimbaled engines, respectively, lb
T_{vac}, $T_{l\,vac}$	rated vacuum thrust of all engines and gimbaled engines, respectively, ft
t	flight time, sec
$V_m(t)$	center-of-gravity velocity of launch vehicle, ft/sec
$V_{mw}(t)$	velocity of launch vehicle relative to wind (defined at center of gravity), ft/sec
$V_w(h)$	wind velocity, ft/sec
x,y	coordinates along X- and Y-body axes, ft
x_a	coordinate locating accelerometer, ft
$x_{c.g.}(t)$	coordinate locating center of gravity, ft
x_n	coordinate locating particular bending-moment station, ft
x_α	coordinate locating angle-of-attack sensor, ft
$\dot{x}_o(t), \dot{y}_o(t)$	components of center-of-gravity velocity vector along X and Y axes, respectively, ft/sec
$\alpha(t)$	rigid-body angle of attack, $\alpha = \theta - \gamma$, radians
$\alpha_s(t)$	angle of attack measured by angle-of-attack sensor, radians

$\alpha_w(t)$	wind induced angle of attack, radians
$\gamma(t)$	flight-path angle, radians
$\delta(t)$	thrust vector (gimbal) angle, radians
$\delta_c(t)$	thrust vector command angle, radians
$n_1(t), n_2(t),$ and $n_3(t)$	control system gain ratios
$\theta(t), \theta_c(t)$	attitude and attitude command angle, respectively, radians
$\theta_f(t)$	feedback angle radians
$\mu_1(t), \mu_2(t)$ and $\mu_3(t)$	control system gain ratios
$\rho(h)$	atmospheric density at altitude h, lb-sec^2/ft^4
$\tau_e(t)$	engine parameter, sec

A dot over a variable indicates a differentiation with respect to time t.

A prime over a variable indicates a differentiation with respect to x.

Axial equation:

$$\ddot{x}_o = \ddot{x}_{c.g.} + \dot{\theta}\dot{y}_o - g \sin \theta + \frac{T_t}{M_t} - \frac{qS_o}{M_t} C_a(M)$$

Lateral equation:

$$\ddot{y}_o = -(\dot{x}_o - \dot{x}_{c.g.})\dot{\theta} - g \cos \theta - \frac{T_1 \delta}{M_t} + \frac{N_\alpha}{M_t}(\alpha + \alpha_w) + \frac{N_{\dot{\theta}}}{M_t}\dot{\theta}$$

$$+ \frac{N_{\dot{\alpha}}}{M_t}(\dot{\alpha} + \dot{\alpha}_w) + \frac{N_{\ddot{\theta}}\ddot{\theta}}{M_t}$$

Pitch equation:

$$\ddot{\theta} = -\frac{\dot{I}_{c.g.}}{I_{c.g.}}\dot{\theta} + \frac{T_1 \kappa_{c.g.}}{I_{c.g.}}\delta + \frac{M_\alpha}{I_{c.g.}}(\alpha+\alpha_w)$$

$$+ \frac{M_{\dot{\theta}}}{I_{c.g.}}\dot{\theta} + \frac{M_{\dot{\alpha}}}{I_{c.g.}}(\dot{\alpha}+\dot{\alpha}_w) + \frac{M_{\ddot{\theta}}}{I_{c.g.}}\ddot{\theta}$$

Gimbaled engined equation:

$$\tau_e\dot{\delta} + \delta = \delta_c$$

Control system equations:

$$\delta_c = a_o\left[(\theta_c-\theta) - \mu_1\dot{\theta} - \mu_2\alpha_s - \mu_3 a_y\right]$$

$$\alpha_s = \alpha + \alpha_w - \frac{(x_\alpha - x_{c.g.})}{V_{mw}}\dot{\theta}$$

$$a_y = \ddot{y}_o + (x_a - x_{c.g_o})\ddot{\theta} + (\dot{x}_o - 2\dot{x}_{c.g.})\theta + g\cos\theta$$

Bending-moment equations:

$$(BM)_n = B_1[\ddot{y}_o + (\dot{x} - 2\dot{x}_{c.g.})\dot{\theta} + g\cos\theta] + [B_2 + B_{\ddot{\theta}}]\ddot{\theta}$$

$$+ B_\alpha[\alpha+\alpha_w] + B_{\dot{\theta}}\dot{\theta} + B_{\dot{\alpha}}[\dot{\alpha}+\dot{\alpha}_w]$$

Miscellaneous equations:

$$V_{mw} = \sqrt{V_m^2 + V_w^2 + 2V_m V_w \cos \gamma}$$

$$V_m = \sqrt{\dot{x}_o^2 + \dot{y}_o^2}$$

$$\alpha_w = \sin^{-1} \left[\frac{V_w \sin \gamma}{V_{mw}}\right]$$

$$\alpha = \tan^{-1} \left[\frac{-\dot{y}_o}{\dot{x}_o}\right]$$

$$\gamma = \theta - \alpha$$

$$h(t) = \int_0^t V_m \sin \gamma \, dt$$

$$r(t) = \int_0^t V_m \cos \gamma \, dt$$

$$q = \frac{1}{2} \rho V_{mv}^2$$

$$T_1 = T_{1vac} - A_1 P_o$$

$$T_t = T_{vac} - (A_1 + A_2) P_o$$

$$M_t = M_o + \dot{M}_t t$$

Equations of motion Coefficients:

(a) Quasi-steady aerodynamics

$$N_\alpha = qS_o \int_0^L C_{n_\alpha}(x,M)\, dx$$

$$N_{\dot\theta} = -\frac{qS_o}{V_{mw}} \int_0^L (x-x_{c.g.})\, C_{n_\alpha}(x,M)\, dx$$

$$N_{\dot\alpha} = 0$$

$$N_{\ddot\theta} = 0$$

$$M_\alpha = qS_o \int_0^L (x-x_{c.g.})\, C_{n_\alpha}(x,M)\, dx$$

$$M_{\dot\theta} = -\frac{qS_o}{V_{mw}} \int (x-x_{c.g.})^2\, C_{n_\alpha}(x,M)\, dx$$

$$M_{\dot\alpha} = 0$$

$$M_{\ddot\theta} = 0$$

Bending-moment coefficients:

(a) Mass

$$B_1 = -\int_{x_n}^L (x-x_n)\, m(x,t)\, dx$$

$$B_2 = -\int_{x_n}^L (x-x_n)(x-x_{c.g.})\, m(x,t)\, dx$$

(b) Quasi-steady aerodynamics

$$B_{\alpha} = qS_o \int_{x_n}^{L} (x-x_n)\, C_{n_\alpha}(x,M)\, dx$$

$$B_{\dot{\theta}} = -\frac{qS_o}{V_{mw}} \int_{x_n}^{L} (x-x_n)(x-x_{c.g.})\, C_{n_\alpha}(x,M)\, dx$$

$$B_{\dot{\alpha}} = 0$$

$$B_{\dot{\theta}^*} = 0$$

APPENDIX C

NUMERICAL FOURIER TRANSFORMS

As indicated in the previous analysis, it is necessary to compute Fourier transforms of the given data. This could well be a formidable task if the data were given in a discrete form $[u(z_i), i=1, \ldots,n]$ and if we had to consider values of the transform variable sufficiently large to cause the integrand to oscillate rapidly. However, the first difficulty may be avoided through the use of smoke-trail methods of wind-velocity measurement and, as far as the second is concerned, the largest value of the wave number k considered in the present example did not cause any serious oscillation of the integrand. True, the size of k was limited by the type of wind data available. However, when continuous wind-velocity readings become available, involving a more refined representation of the wind profile and, thus, larger values of k, the response properties of the vehicle will most likely place an upper limit on the values of k which need be considered. Thus, it will still be possible to use a relatively simple program for the computation of the necessary Fourier transforms.

Single Fourier Transform

By definition

$$U(k) = \int_0^D u(z)\, e^{-ikz}\, dz \qquad (C-1)$$

since it is assumed that

$$u(z) = 0 \quad \text{for} \quad z<0 \quad \text{or} \quad z>D \qquad (C-2)$$

However, noting that u(z) is defined only at the equidistant points z_n, n=1,..., N where

$$z_n = (n-1)\Delta z$$
$$z_N = D \qquad (C-3)$$

Eq. (C-1) is rewritten as

$$U(k) = \sum_{n=1}^{N-1} \int_{z_n}^{z_{n+1}} u(z)\, e^{-ikz}\, dz \qquad (C-4)$$

and u(z) is assumed to be linear between the points z_n and z_{n+1}, i.e.

$$u(z) = a_n\, z_n + b_n \qquad (C-5)$$

where

$$a_n = [u(z_{n+1}) - u(z_n)]/\Delta z$$
$$b_n = n\, u(z_n) - (n-1)\, u(z_{n+1}) \qquad (C-6)$$

For computation purposes Eq. (C-4) is rewritten in terms of real and imaginary expressions.

$$U(k) = \sum_{n=1}^{N-1} [R^n(k) - iI^{(n)}(k)] \qquad \text{(C-7)}$$

where

$$R^n(k) = \int_{z_n}^{z_{n+1}} u(z) \cos(kz)\, dz$$

and (C-8)

$$I^n(k) = \int_{z_n}^{z_{n+1}} u(z) \sin(kz)\, dz$$

The expression (C-5) is then substituted for u(z) into Eq. (C-8) and, after simplification, the following results are obtained:

$$R^n(k) = \Delta z \left\{ [u(z_{n+1}) - u(z_n)] \frac{\sin 2(n-1)\alpha}{2\alpha} + \frac{\sin\alpha}{\alpha} [u(z_{n+1}) \cos(2n-1)\alpha - (u(z_{n+1}) - u(z_n)) \frac{\sin(2n-1)\alpha}{2\alpha} \right\} \qquad \text{(C-9)}$$

$$I^n(k) = \Delta z \left\{ -[u(z_{n+1}) - u(z_n)] \frac{\cos 2(n-1)\alpha}{2\alpha} + \frac{\sin\alpha}{\alpha} [(u(z_{n+1}) - u(z_n)) \frac{\cos(2n-1)\alpha}{2\alpha} + u(z_{n+1}) \sin(2n-1)\alpha] \right\} \qquad \text{(C-10)}$$

where $\alpha = k\Delta z/2$.

Thus Eqs. (C-9) and (C-10), along with Eq. (C-7), constitute the solution of the problem.

Double Fourier Transform

The double Fourier transform is computed by using the previous results twice. Using Eqs. (18 a) and (C-2)

$$\Phi_{uu}(k_1,k_2) = \int_0^D\int_0^D \varphi_{uu}(z_1,z_2)\, e^{i(k_1z_1-k_2z_2)}\, dz_1dz_2 \qquad (C\text{-}11)$$

or, rewriting in terms of sums

$$\Phi_{uu}(k_1,k_2) = \sum_{r=1}^{N-1}\sum_{s=1}^{N-1} \int_{z_r}^{z_{r+1}}\int_{z_s}^{z_{s+1}} \varphi_{uu}(z_1,z_2)e^{i(k_1z_1-k_2z_2)}dz_1dz_2$$

$$= \sum_{r=1}^{N-1} \int_{z_r}^{z_{r+1}} \Big[\sum_{s=1}^{N-1} \int_{z_s}^{z_{s+1}} \varphi_{uu}(z_1,z_2)e^{-ik_2z_2}dz_2\Big]e^{ik_1z_1}dz_1 \qquad (C\text{-}12)$$

Noting Eqs. (C-4) and (C-7), Eq. (C-12) is rewritten as

$$\Phi_{uu}(k_1,k_2) = \sum_{r=1}^{N-1} \int_{z_n}^{z_{r+1}} \Big[\sum_{s=1}^{N-1} (R^s(z_1,k_2)-iI^s(z_1,k_2))\Big]e^{ik_1z_1}dz_1 \qquad (C\text{-}13)$$

where

$$R^s(z_1,k_2) = \int_{z_s}^{z_{s+1}} \varphi_{uu}(z_1,z_2)\cos k_2z_2dz_2$$

and (C-14)

$$I^s(z_1,k_2) = \int_{z_s}^{z_{s+1}} \varphi_{uu}(z_1,z_2)\sin k_2z_2dz_2$$

Thus Eqs. (C-9) and (C-10) may be used to compute the above expressions with $u(z_{n+1})$ and $u(z_n)$ being replaced by $\varphi_{uu}(z_r, z_{s+1})$ and $\varphi_{uu}(z_r, z_s)$, respectively. Finally, it is noted that Eq. (C-13) is a single Fourier transform in z_1 and the previous results are again applied.

Check

In order to check the accuracy of the previous analysis, the above expressions were used to compute the inverse transforms also. The results were in good agreement. This analysis was used to determine the Δk interval required in the numerical integrations.

REFERENCES

1. H.C. Lester and D.F. Collins, "Determination of Loads on a Flexible Launch Vehicle During Ascent Through Winds", NASA TN D-2590, February 1965.

2. N. Sissenwine, "Wind Shear and Gusts for Design of Guidance Systems for Vertically Rising Air Vehicles", Air Force Surveys in Geophysics, No. 57, AFCRC-TN-58-216, November 1954.

3. N. Sissenwine, "A Review - Tropospheric Wind Profiles in Aerospace Vehicle Design", First AIAA Annual Meeting, Washington, D.C., June 29-July 2, 1964 (AIAA Paper No. 64-315).

4. N.P. Hobbs, E.S. Criscione and M. Ayvazian, "Simplified Analytical Methods for Use in Preliminary Design of Vertically-Rising Vehicles Subjected to Wind Shear Loads, Part 1, Evaluation of Methods", Technical Documentary Report No. FDL-TDR-64-8, Part 1, August 1964.

5. F.P. Beer and W.C. Lennox, "Determination of the Survival Probability a Launch Vehicle Rising Through a Random Wind Field", to be published in the Jouranl of Spacecraft and Rockets, March-April, 1966.

6. J.C. Houbolt, R. Steiner and K.G. Pratt, "Dynamic Response of Airplanes to Atmospheric Turbulence Including Flight Data on Input and Response", NASA TR R-199, June 1964.

7. R.E. Bieber, "Missile Structural Loads by Nonstationary Statistical Methods", Journal of the Aerospace Sciences, Vol. 28, No. 4, April 1961.

8. W.W. Vaughan, "Interlevel and Intralevel Correlations of Wind Components for Six Geographical Locations", NASA TN D-561, December 1960.

9. V.V. Solodovnikov, Introduction to the Statistical Dynamics of Automatic Control Systems, Dover Publications, Inc., New York, New York, 1960, p. 10.

10. D.G.B. Edelen, "On the Dynamical Effects of Fuel Flow on the Motion of Boost Vehicles", Memo. RM-3268-NASA, (Contract No. NASr-21(03)), the RAND Corp., October,1962.

11. E.T. Whittaker, A Treatise on the Analytical Dynamics of Particles and Rigid Bodies, Fourth ed., Dover Publications, New York, New York, 1944.

12. D.R. Lukens, A.F. Schmitt and G.T. Broucek, "Approximate Transfer Functions for Flexible-Booster-and-Autopilot-Analysis", WADD TR-61-93, U.S. Air Force, April 1961.

13. R.L. Bisplinghoff, H. Ashley and R.L. Halfman, Aeroelasticity, Addison-Wesley Pub. Co., Inc., Cambridge, Mass., 1955.

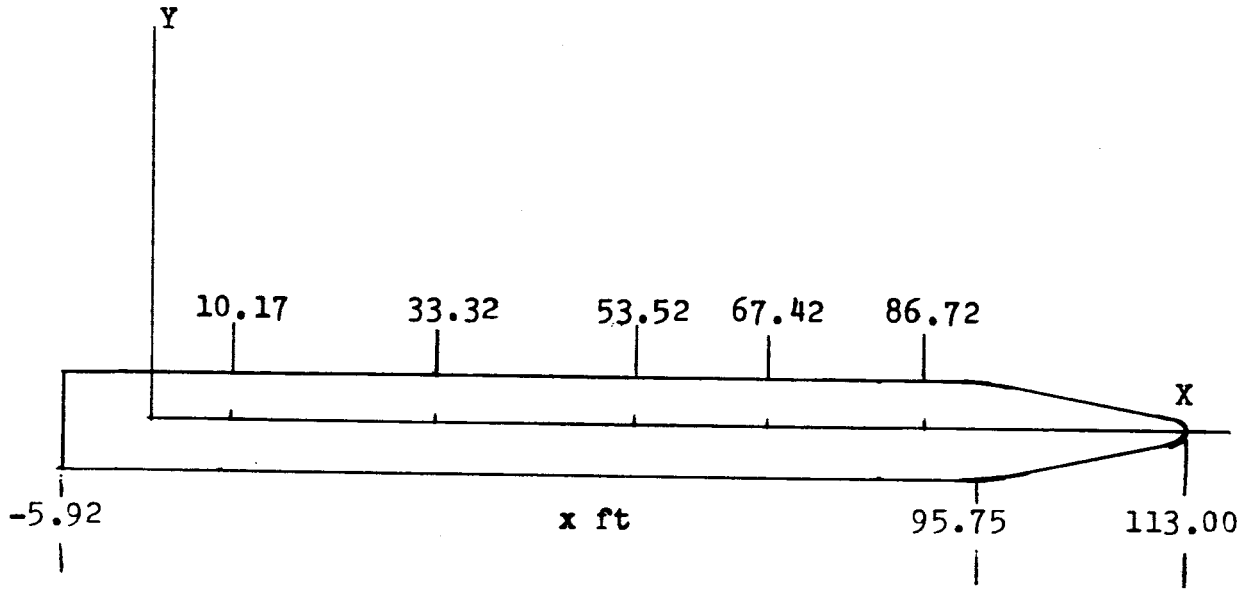

LOCATION OF BENDING MOMENT STATIONS

Figure 1

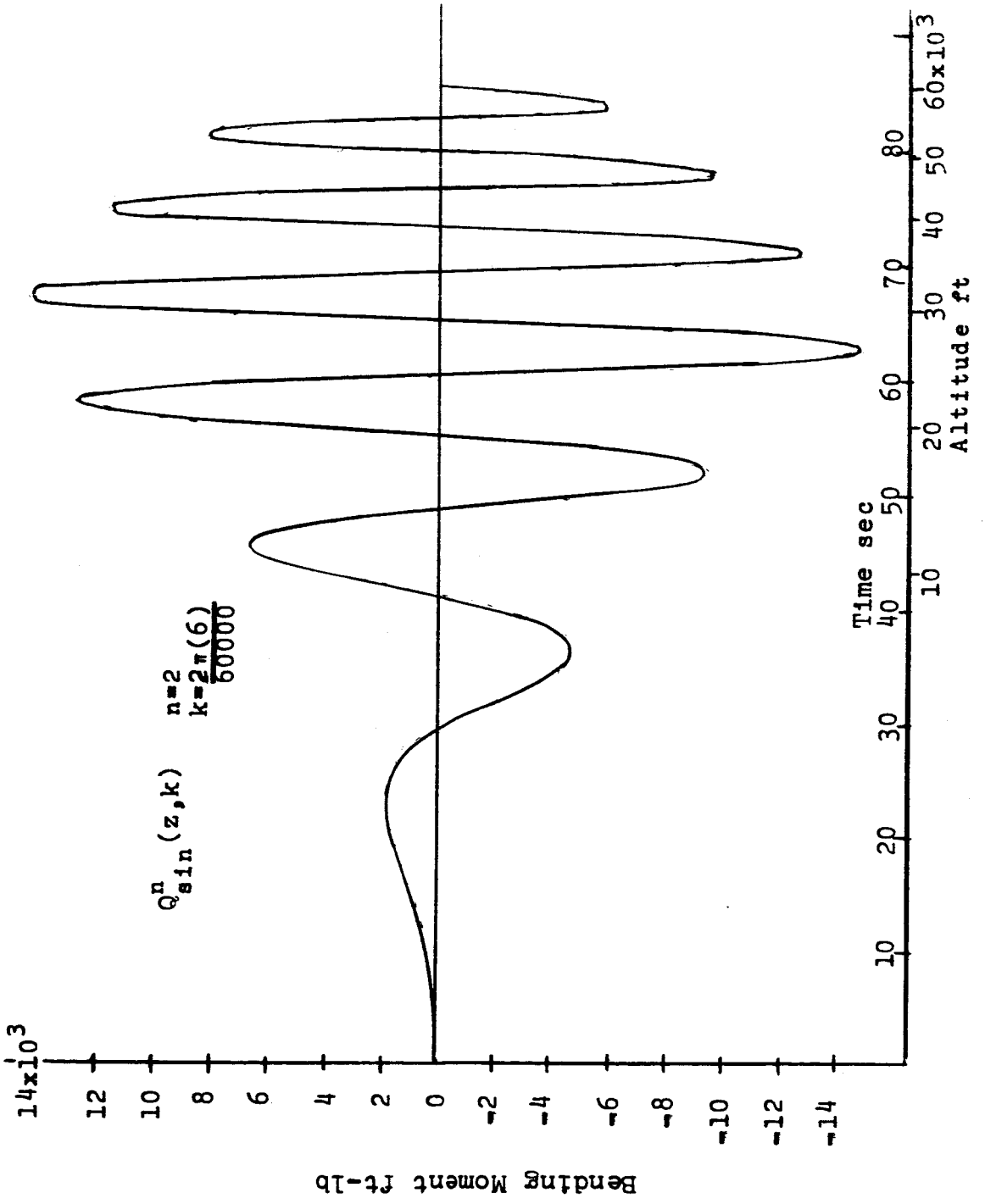

BENDING MOMENT RESPONSE

FIGURE 2a

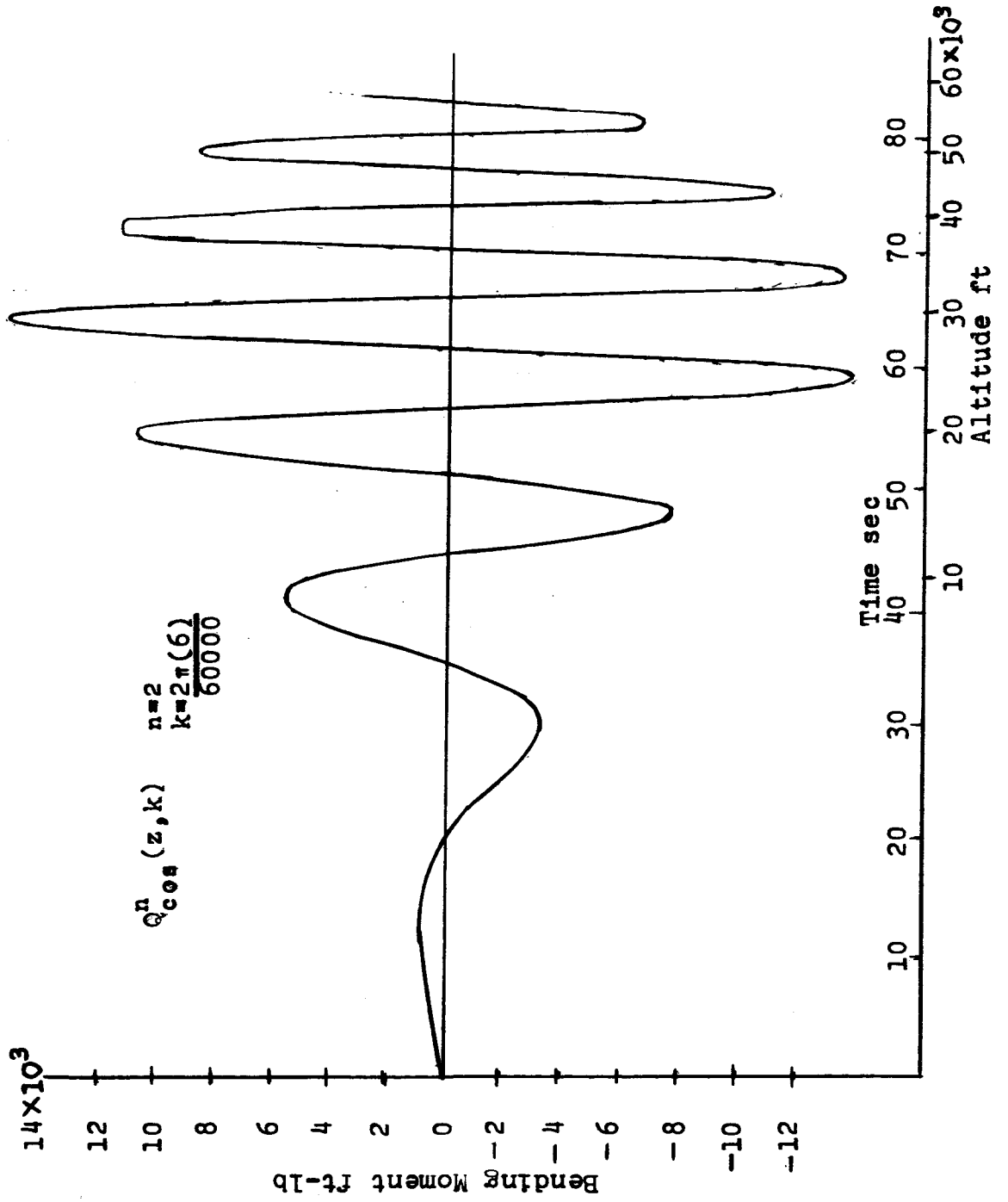

BENDING MOMENT RESPONSE

FIGURE 2b

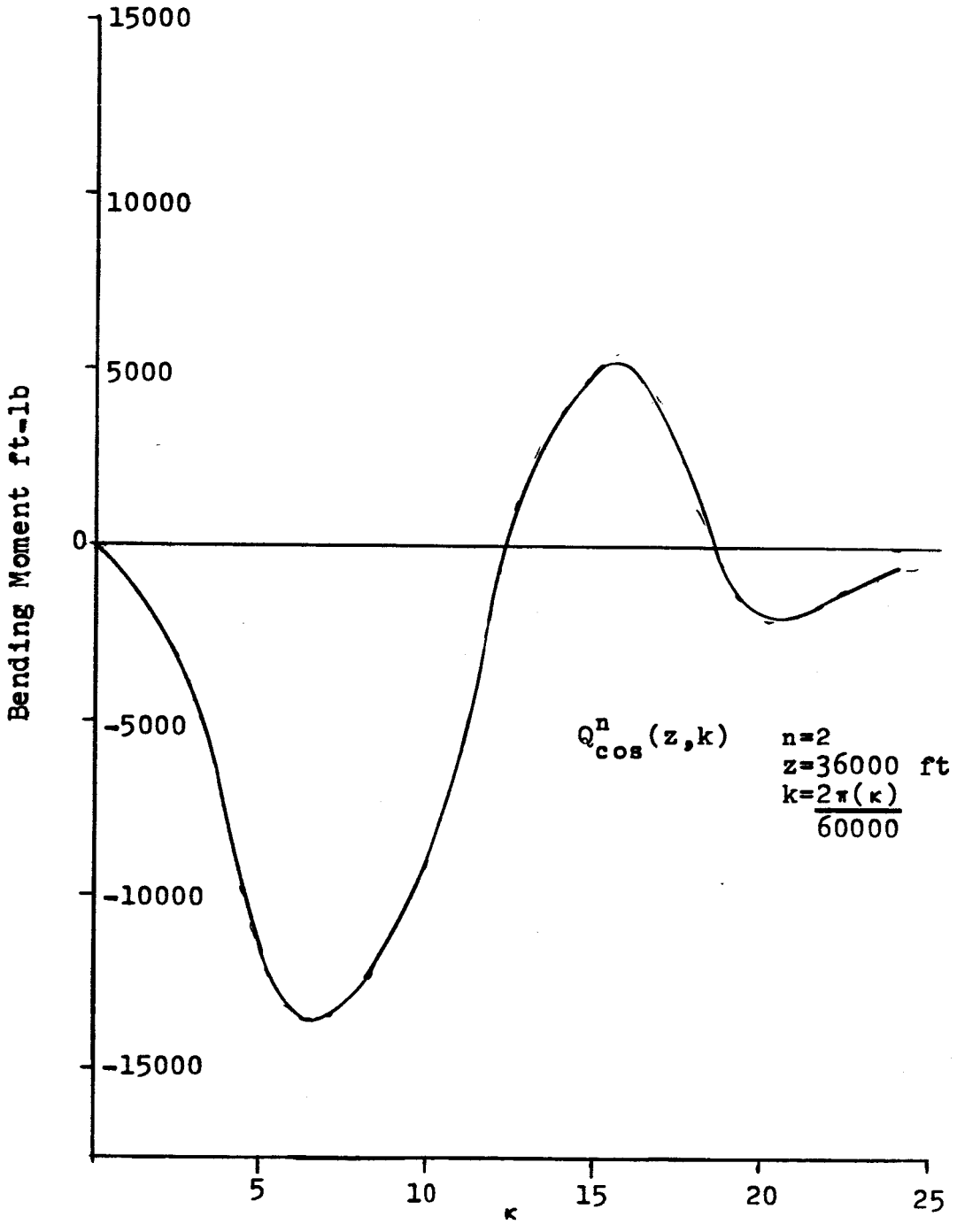

BENDING MOMENT RESPONSE

FIGURE 3

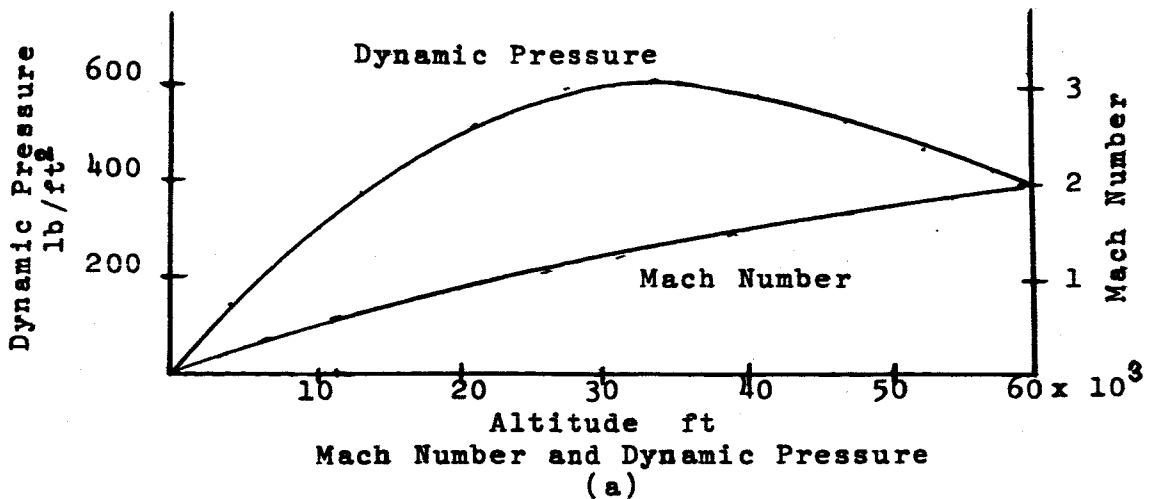

Mach Number and Dynamic Pressure

(a)

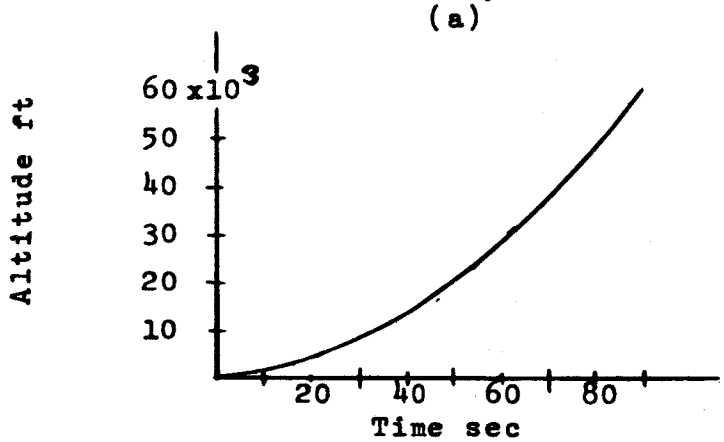

(b)

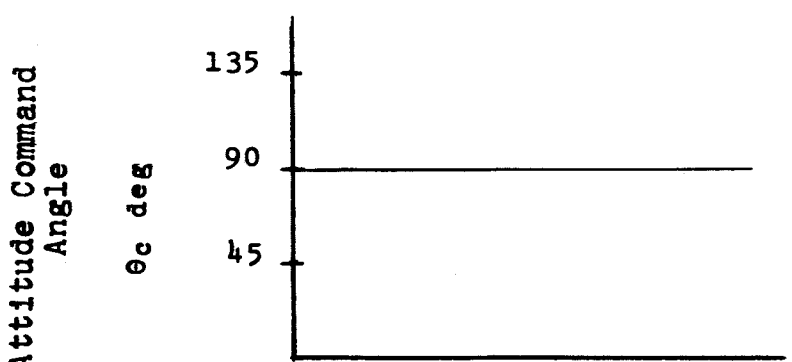

Pitch Program

(c)

ZERO-WIND TRAJECTORY DATA FOR VERTICAL ASCENT

FIGURE 4

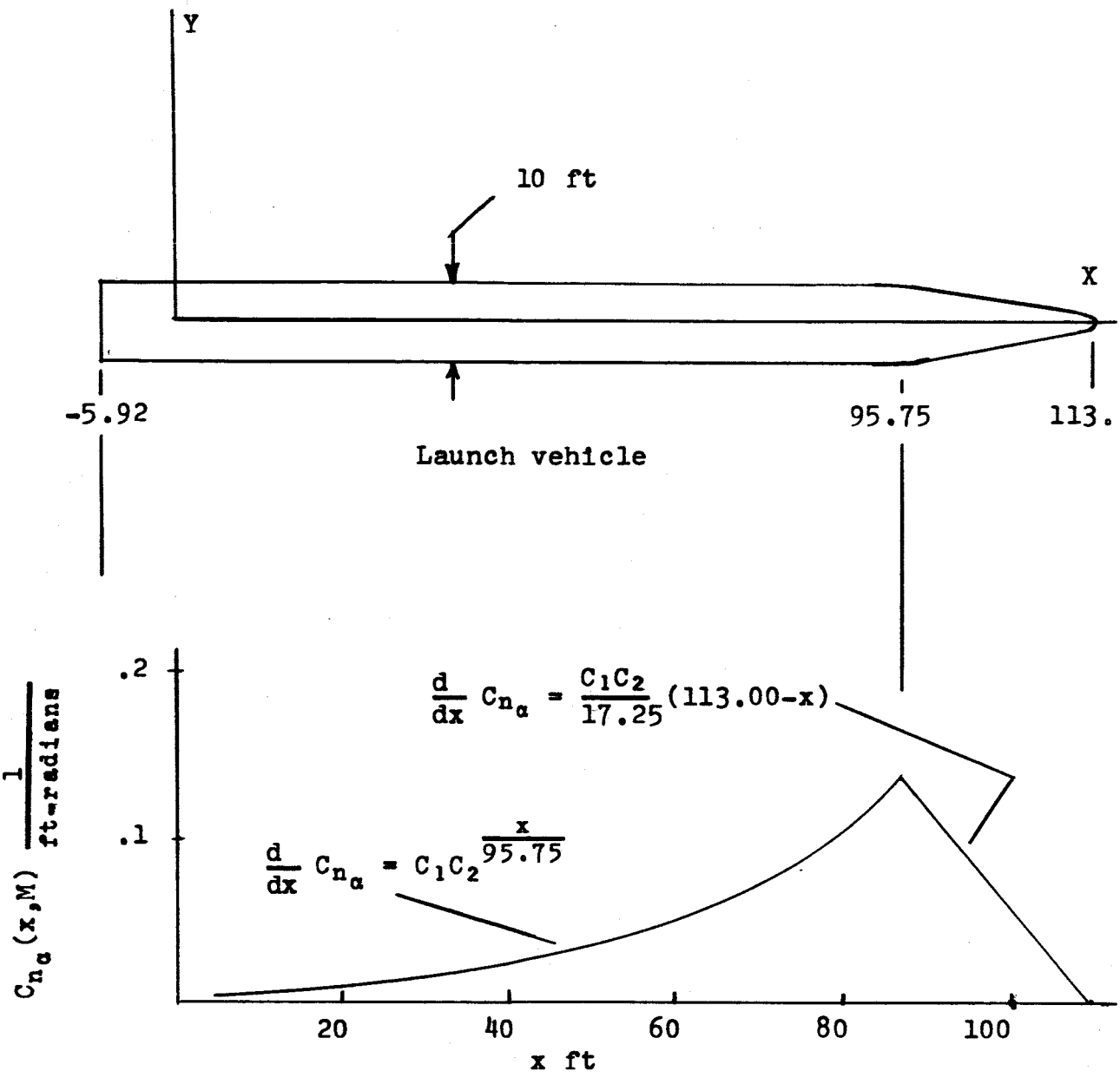

ASSUMED NORMAL-FORCE DISTRIBUTION M=2.0

FIGURE 5

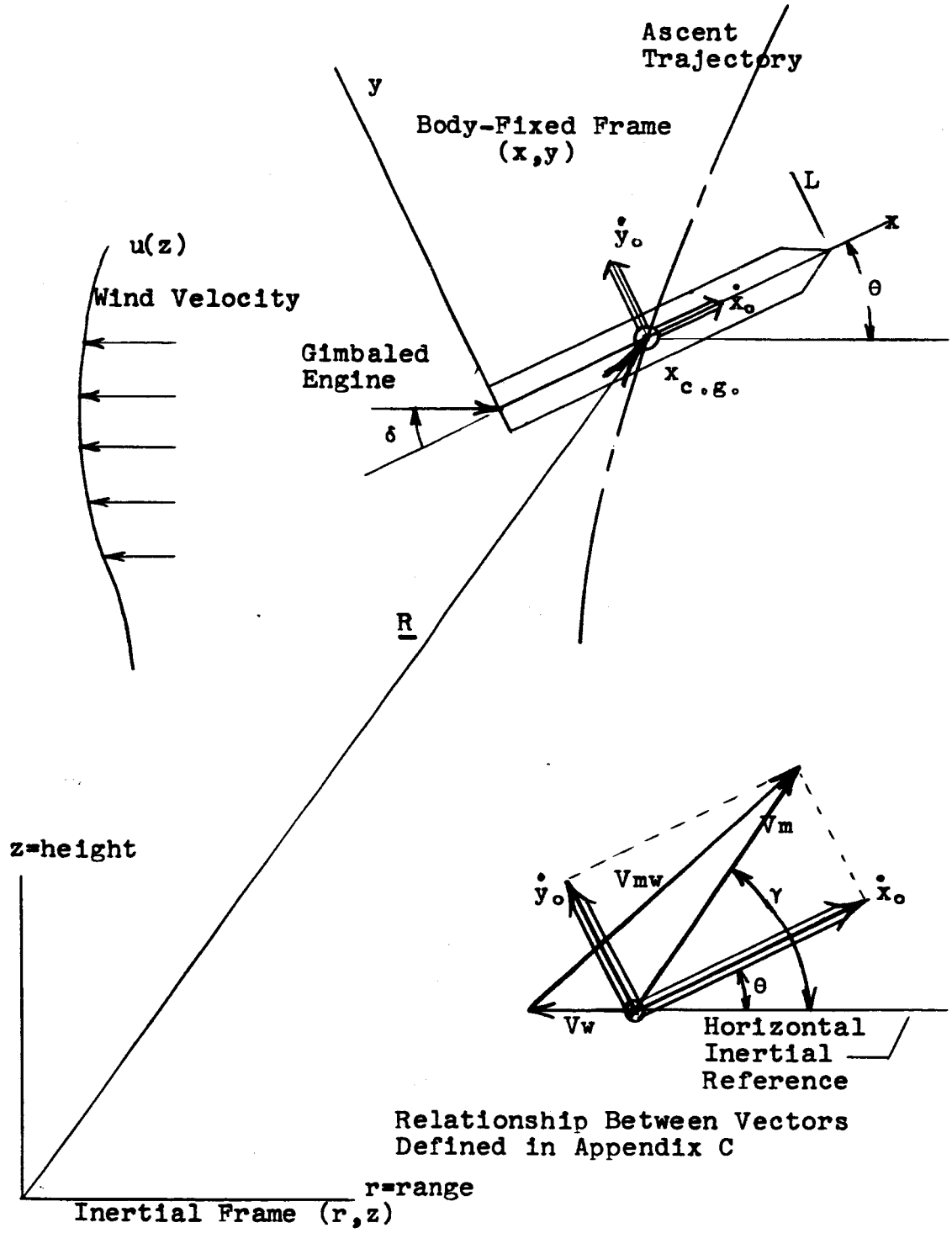

Relationship Between Vectors
Defined in Appendix C

COORDINATE SYSTEM FOR LAUNCH VEHICLE PROBLEM

FIGURE 6

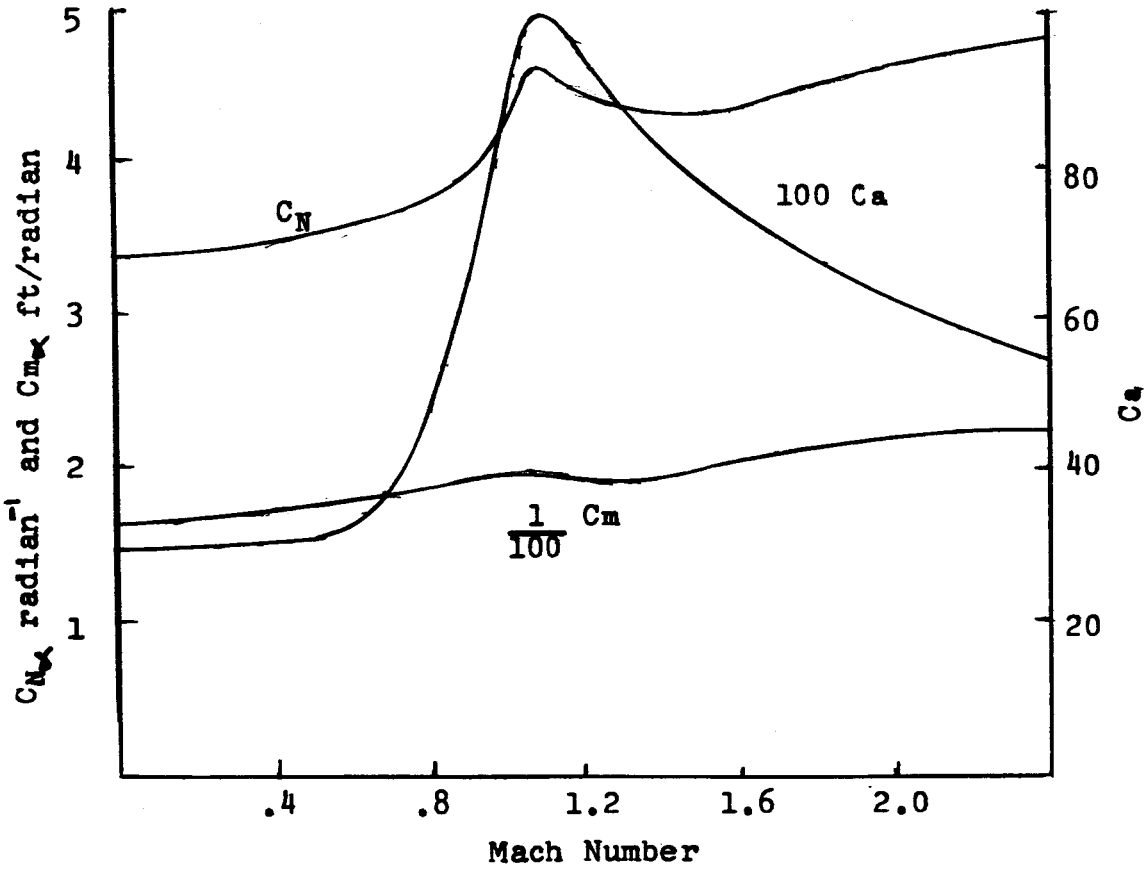

AERODYNAMIC DATA

FIGURE 7

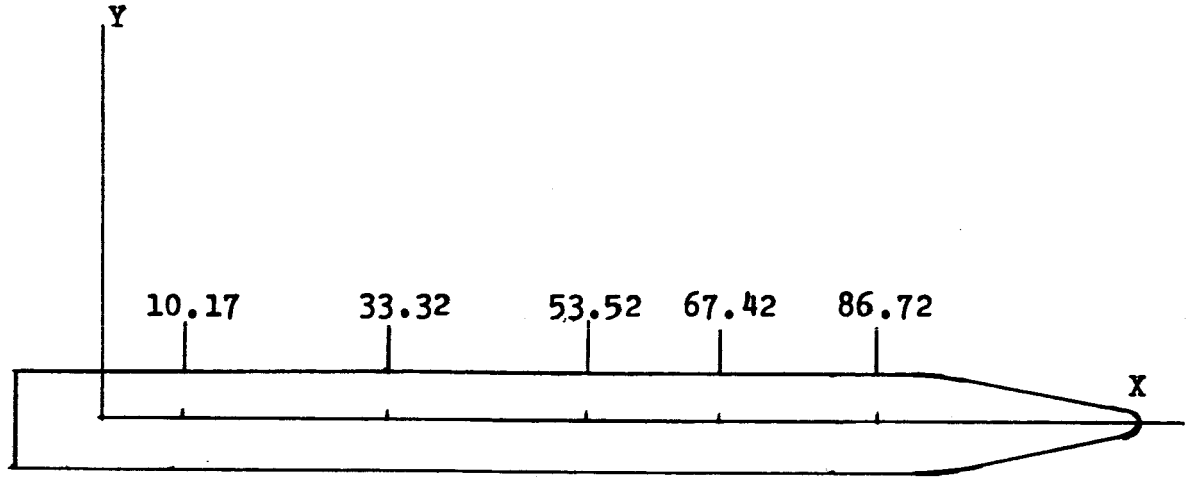

Location of Bending Moment Stations

(a)

n	Location ft	Mean ft-lb	Standard Deviation ft-lb
1	10.17	8,698	45,454
2	33.32	19,710	109,290
3	53.50	12,551	84,322
4	67.42	9,981	52,884
5	86.72	2,690	15,181

Bending Moment Response at 36,000 ft

(b)

RESULTS

FIGURE 8

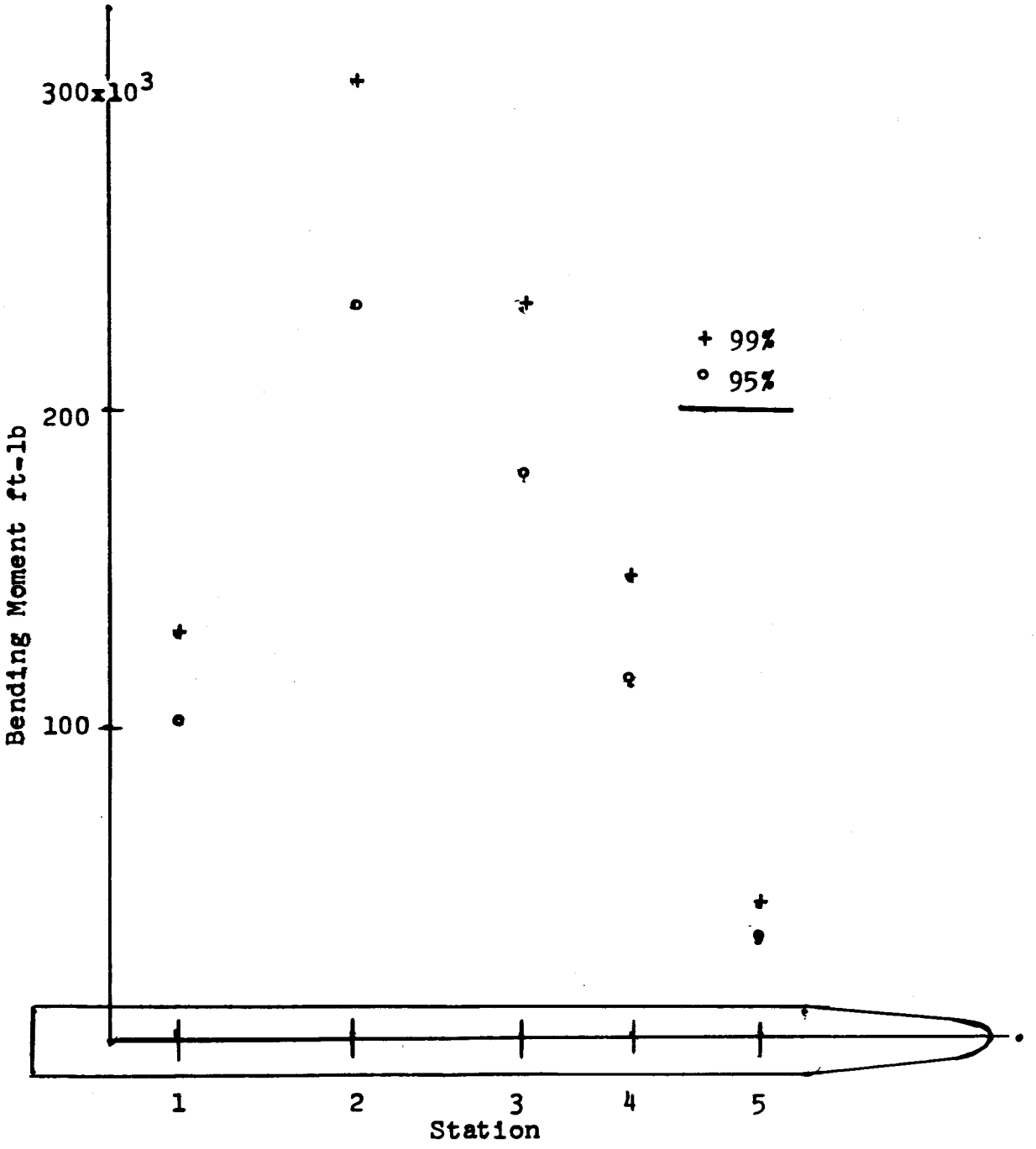

COMPARISON OF 95 AND 99% EXTREME VALUE BENDING MOMENTS
ALTITUDE = 36,000 ft

FIGURE 9

BENDING MOMENT AT STATION n=2 DUE TO
INPUTS OF THE FORM $u(z)=C\sin(kz)$

	C=1	C=10	C=100
Altitude ft		Bending Moment ft-lb	
10,000	$-.57001\times10^{4}$	$-.57101\times10^{5}$	$-.57889\times10^{6}$
15,000	$.31386\times10^{3}$	$.31887\times10^{4}$	$.31685\times10^{5}$
20,000	$.12733\times10^{5}$	$.12734\times10^{6}$	$.12650\times10^{7}$
25,000	$.79084\times10^{4}$	$.78808\times10^{5}$	$.80087\times10^{6}$
30,000	$-.12200\times10^{5}$	$-.12361\times10^{6}$	$-.11987\times10^{7}$
35,000	$-.12856\times10^{5}$	$-.12498\times10^{6}$	$-.12627\times10^{7}$
40,000	$.17321\times10^{5}$	$.17476\times10^{6}$	$.17078\times10^{7}$
45,000	$.92296\times10^{4}$	$.91845\times10^{5}$	$.92593\times10^{6}$
50,000	$.44638\times10^{4}$	$.44203\times10^{5}$	$.45153\times10^{6}$

LINEARITY CHECK

TABLE 1

ALTITUDE km	MEAN ft/sec	STANDARD DEVIATION ft/sec
0	0.93	9.27
1	0.62	20.89
2	7.35	22.34
3	13.94	25.32
4	19.91	28.80
5	25.82	33.33
6	31.49	38.41
7	37.40	43.34
8	43.86	48.45
9	50.07	55.01
10	56.89	61.77
11	63.94	67.58
12	69.06	71.09
13	69.94	71.34
14	64.66	67.44
15	54.86	66.55
16	42.29	52.95
17	20.00	47.20
18	14.86	36.87
19	6.23	26.66
20	2.21	11.92

EAST-WEST WIND VELOCITY STATISTICS

TABLE 2

TABLE 3

0	1.00								15	1.00					
1	.690	1.00							16	.919	1.00				
2	.616	.830	1.00						17	.864	.905	1.00			
3	.555	.706	.881	1.00					18	.819	.856	.896	1.00		
4	.504	.617	.791	.913	1.00				19	.776	.811	.824	.869	1.00	
5	.452	.542	.725	.849	.931	1.00			20	.726	.771	.782	.802	.864	1.00
6	.408	.484	.678	.805	.888	.944	1.00			15	16	17	18	19	20
7	.372	.429	.631	.764	.850	.908	.951	1.00							
8	.334	.380	.583	.729	.817	.877	.919	.956	1.00						
9	.309	.350	.550	.693	.783	.847	.887	.924	.958	1.00					
10	.285	.309	.513	.662	.752	.814	.857	.897	.932	.961	1.00				
11	.253	.265	.487	.630	.722	.786	.832	.862	.906	.934	.957	1.00			
12	.224	.242	.453	.606	.694	.759	.809	.851	.885	.906	.927	.958	1.00		
13	.206	.229	.434	.584	.680	.743	.792	.834	.864	.879	.897	.923	.949	1.00	
14	.197	.220	.426	.579	.671	.734	.781	.815	.846	.859	.870	.889	.913	.945	1.00
15	.195	.208	.411	.571	.665	.727	.773	.806	.831	.835	.843	.859	.882	.907	.934
16	.189	.202	.407	.556	.645	.706	.745	.779	.803	.803	.807	.821	.842	.867	.887
17	.183	.195	.389	.531	.619	.678	.711	.744	.765	.759	.766	.778	.788	.810	.832
18	.160	.169	.356	.491	.576	.634	.663	.712	.722	.718	.722	.734	.739	.759	.789
19	.129	.123	.303	.437	.519	.580	.614	.649	.668	.668	.666	.684	.687	.710	.746
20	.110	.073	.249	.375	.454	.513	.555	.587	.613	.618	.623	.633	.642	.665	.700
Altitude km	0	1	2	3	4	5	6	7	8	9	10	11	12	13	14

CORRELATION COEFFICIENTS OF EAST-WEST WIND VELOCITY